



## Laundry wastewater treatment by peroxi-coagulation

Tulin Yilmaz Nayir<sup>a,\*</sup>, Ozge Dinc<sup>b</sup>, Serdar Kara<sup>a</sup>, Abdurrahman Akyol<sup>a</sup>, Anatoli Dimiglo<sup>c</sup>

<sup>a</sup>Department of Environmental Engineering, Gebze Technical University, 41400 Gebze, Kocaeli, Turkey,  
email: tulinyilmaz@gtu.edu.tr (T.Y. Nayir)

<sup>b</sup>Institute of Health Science, Department of Biotechnology, The University of Health Science, 34668 Istanbul, Turkey

<sup>c</sup>Department of Environmental Engineering, Duzce University, Konuralp Yerleşkesi, 81620 Duzce, Turkey

Received 16 May 2019; Accepted 15 November 2019

---

### ABSTRACT

Peroxi-coagulation (PC) process was developed with iron anodes and carbon-polytetrafluoroethylene cathodes for the treatment of laundry wastewater (LWW). The effect of operating conditions as pH, current density and temperature were investigated by response surface modeling. Whereas temperature change did not affect the reaction, pH change dominated it especially between pH 5–7 causing an effective coagulation process. The model was devoted to maximizing the removal of chemical oxygen demand (COD), methylene blue substances (MBAS) and total phosphorus (TP) and to minimizing total residual iron (TFe) concentration in the treated wastewater. Complete TP removal and high removal efficiencies in terms of COD and MBAS were provided at optimal operation conditions (pH 7, current density 45 mA/cm<sup>2</sup> and temperature: 25°C). During the PC process H<sub>2</sub>O<sub>2</sub> and S<sub>2</sub>O<sub>8</sub><sup>2-</sup> production was observed. According to the results, H<sub>2</sub>O<sub>2</sub> concentration was stable during the process after a certain increment; however, persulfate production reached maximum value when surfactant (namely: linear alkylbenzene sulfonate) concentration was almost minimum in the bulk. In the PC process, both the oxidation with possibly formed radicals (i.e. \*OH and SO<sub>4</sub>\*-) and the coagulation with iron precipitation are responsible for the LWW treatment.

*Keywords:* Peroxi coagulation; Laundry wastewater; Response surface modeling; Surfactant; Persulfate

---

### 1. Introduction

Industrial laundries discharge a significant amount of wastewater as a result of washing tons of dirty clothes. Laundry wastewater (LWW) is composed of organic and inorganic compounds such as greases, surfactants, oils, pesticides, phenols as organic content and pH, sulfur, chlorides, alkalinity, toxic compounds as inorganic content [1]. Most of the organic and inorganic compounds were below the maximum limits in accordance with the environmental legislation that pH, chemical oxygen demand (COD), total phosphorus (TP) and surfactant concentrations were mostly analyzed. The LWW contains COD concentration between 275–4,800 mg/L, phosphate concentration between 0.4–95 mg/L and surfactant concentration between 1 and

1,024 mg/L [2–6]. Wastewater quantity differs depending on the dosage of detergents, bleach and cleaning aids, which may vary depending on whether the contaminated articles originate from homes, hotels or hospitals. Moreover, surfactants as the main surface-active reagents of the detergents are important pollutants in the LWWs.

Previous studies have been conducted for either specific surfactant removal or LWW treatment such as biological treatment [7,8], electrocoagulation/electroflotation [9], ozonation [10], coagulation and membrane filtration [11,12] and electro-peroxone process [3]. Among those processes, electrochemical treatment techniques have been drawn attention with their easy operation and less sludge production properties. In electrocoagulation process while the anode

---

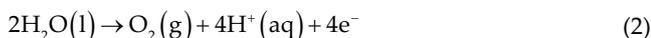
\* Corresponding author.

electrode (iron or aluminum) is producing ions for flocculation, the cathode electrode generates hydrogen gas for flotation of contaminants. In case of electrooxidation, insoluble electrodes are used to oxidize pollutants directly by active oxygen like hydroxyl radicals ( $\cdot\text{OH}$ ) and/or indirectly in the existence of chlorine ions. In this context, peroxi-coagulation (PC) is one of the electrochemical treatment processes that work like a combination of electrocoagulation and electrooxidation in the same reactor simultaneously.

Although the first studies on the PC process have been started a few decades ago [13,14], there are limited studies for environmental applications. These studies can be given such as composite wastewater treatment with iron electrodes and externally added  $\text{H}_2\text{O}_2$  [15], phenol treatment with steel anode and graphite cathode [16], herbicides degradation with  $\text{O}_2$ -fed cathode and iron anode [17,18], acrylonitrile removal with graphite felt cathode and iron anode [19], textile dye degradation with carbon-polytetrafluoroethylene (PTFE) and iron electrodes [20–23], sodium dodecyl sulfate removal with iron electrodes and externally added  $\text{H}_2\text{O}_2$  [24].

The PC provides degradation of pollutants with electro-generated  $\cdot\text{OH}$  and coagulation with  $\text{Fe}(\text{OH})_3$  precipitate. In this process, following reactions may occur [16] at the electrode surfaces and/or in the bulk solution.

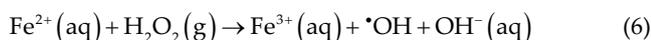
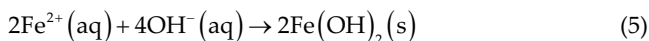
At anode:



At cathode:

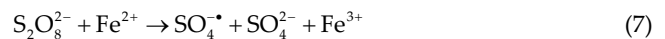


In the bulk:



As it is seen from the well-known Fenton reaction (6),  $\cdot\text{OH}$  radicals are generated in the bulk solution and ferrous iron is oxidized to ferric iron. While ferrous iron is supplied from the anode iron electrodes,  $\text{H}_2\text{O}_2$  is produced through reaction (4) at the cathode. The oxygen requirement for this reaction can be provided from the reaction (2) or external  $\text{O}_2$  dosage. Excess  $\text{Fe}^{3+}$  ions which are produced in reaction (6) precipitates as  $\text{Fe}(\text{OH})_3$ . Thus, pollutants can be removed by a combination of coagulation with  $\text{Fe}(\text{OH})_3$  and oxidation with generated  $\cdot\text{OH}$  radicals [16,19,25]. Moreover, it is known that when surfactants containing wastewaters are electrolyzed, persulfates can be produced from the sulfate ions which are degradation products of sodium dodecyl sulfate [26]. Persulfate ( $\text{S}_2\text{O}_8^{2-}$ ) is a newly emerging oxidant ( $E^0 = 2.01 \text{ V}$ ) for water and wastewater treatment processes and it can be activated to generate more powerful oxidant  $\text{SO}_4^{\cdot-}$  ( $E^0 = 2.60 \text{ V}$ ) [27]. Heat-UV radiation, electrolysis ozone

and electron transfer between transition metals methods are used for persulfate activation [28]. In the transition metals method, persulfate can be activated through one-electron transfer using metals such as silver, copper, iron, zinc, cobalt, and manganese. Among these metals, iron has been used effectively in the activation of persulfate ion, since it is relatively non-toxic, environmentally, friendly and more cost-effective metal than other transition metals [29]. Activation of persulfate ion occurs according to reaction (7). To get ferrous ion more than sufficient concentration for reaction with persulfate causes scavenging the sulfate radical through reaction (8) [28,29].



This study focused on the treatment of LWW by the PC process equipped with carbon-PTFE cathode and iron sheet anode. An integrated approach was developed by an experimental design for maximizing the removal of COD, anionic surfactant methylene blue substances (MBAS) and TP from LWW while minimizing the (TFe) concentration in the bulk solution. The effects of controlling factors of the PC process as current density, initial pH and temperature individually and their interactions on LWW treatment were evaluated. In-situ persulfate and hydrogen peroxide production were also observed to find the effect of oxidants produced in the PC system.

## 2. Materials and methods

### 2.1. LWW characterization

LWW was obtained from an industrial laundry effluent at different times and stored at  $4^\circ\text{C}$ . Samples were analyzed within 24 h and characterization are given in Table 1.

### 2.2. Experimental set-up

The PC process was performed in a plexiglass reactor with the dimensions of  $10 \text{ cm} \times 10 \text{ cm} \times 10 \text{ cm}$ . An iron sheet with  $36 \text{ cm}^2$  active area was used as an anode. Two pieces of carbon-PTFE cathodes in same area with the anode were used

Table 1  
Characterization of laundry wastewater

Parameter	Value
pH	11.8–12.3
Electrical conductivity (mS/cm)	1.5–2.5
COD (mg/L)	720–1,170
Anionic surfactant (mg/L)	31–75
Turbidity (NTU)	103–117
Suspended solids (mg/L)	75–100
Sulphate (mg/L)	90–95
Total nitrogen (mg/L)	2–5
Total phosphorus (mg/L)	35–60

as cathode and the cathodes were prepared same as previous study [3]. The electrodes were placed with a gap of 1 cm between them in an electrode holder (Fig. 1) that designed to place electrodes, pH and  $H_2O_2$  probes during the operations. For each run, 800 mL of laundry effluent was poured into the reactor. When the PC process was started, the wastewater in the reactor was mixed to provide both homogeneous reaction conditions and oxygenate the LWW. Samples were taken at regular intervals during 30 min operation time and filtered through 0.45  $\mu\text{m}$  filter for further analysis.

### 2.3. Analytical methods

COD, MBAS and suspended solids were determined according to the Standard Methods procedure [30]. pH/conductivity and turbidity measurements were carried out by multiparameter (Mettler Toledo S700, Switzerland) and turbidimeter (Hach 2100Q, USA), respectively. Total nitrogen, TP and TFe were determined by using cuvette tests (Hach Lange, Germany) LCK 138, LCK 350 and USEPA FerroVer method, respectively. Hydrogen peroxide concentration was followed during the process by using Jumo GmbH & Co. (Germany) analyzer. Persulfate ions were measured according to the method in [31]. In this method, 2.5 N  $H_2SO_4$  and 0.4 N FAS were added and allowed to react for 40 min. Then, 0.6 N  $NH_4SCN$  solutions was added and concentration was measured at 450 nm wavelength in spectrophotometer (Hach Lange DR5000, Germany) through a pre-established calibration curve.

### 2.4. Mathematical and statistical procedures

Response surface modelling (RSM) combined with Box–Behnken experimental design was used for the optimization of the LWW treatment by the PC process. While the controlling factors of the process (independent variables) were current density ( $A$ ), pH ( $B$ ) and temperature ( $C$ ), dependent variables (responses) of the PC process were TP ( $R_1$ ), MBAS ( $R_2$ ), COD ( $R_3$ ) and TFe ( $R_4$ ). A second-order polynomial model was used for the regression analysis.

In Eq. (9),  $R$  is the response,  $\beta_0$  is the intercept,  $\beta$  values signify coefficients and,  $x$  values are the independent factors.

$$R = \beta_0 + \beta_1x_1 + \beta_2x_2 + \beta_3x_3 + \beta_{12}x_1x_2 + \beta_{13}x_1x_3 + \beta_{23}x_2x_3 + \beta_{11}x_1^2 + \beta_{22}x_2^2 + \beta_{33}x_3^2 \quad (9)$$

The experimental design was established with the value calculated from the average of minimum and maximum values. Actual values of the variables for the coded values are given in Table 2. Design expert package, version 11 (STAT-EASE Inc., Minneapolis, USA) was used for the design of experimental parameters.

## 3. Results and discussion

### 3.1. Box–Behnken design and model equation prediction

Box–Behnken experimental design that is given in Table 3 has been used for optimizing the controlling factors of the PC process. COD, MBAS and TP results were stated as a ratio of final concentration ( $C$ ) at the end of the each run to the corresponding initial concentration ( $C_0$ ).

Analysis of variance (ANOVA) test was conducted to define the significance of the model and significant model terms. Significance of the models was determined according to Fisher variation values ( $F$ -value), probability value ( $p$ -value) and adequate precision. ANOVA results (Table 4) showed that the quadratic models were significant for each

Table 2  
Actual values of the variables for the coded values

Variables	Actual values for the coded values		
	-1	0	1
Current density ( $\text{mA}/\text{cm}^2$ )	15	30	45
Initial pH	3	7	11
Temperature ( $^{\circ}\text{C}$ )	25	35	45

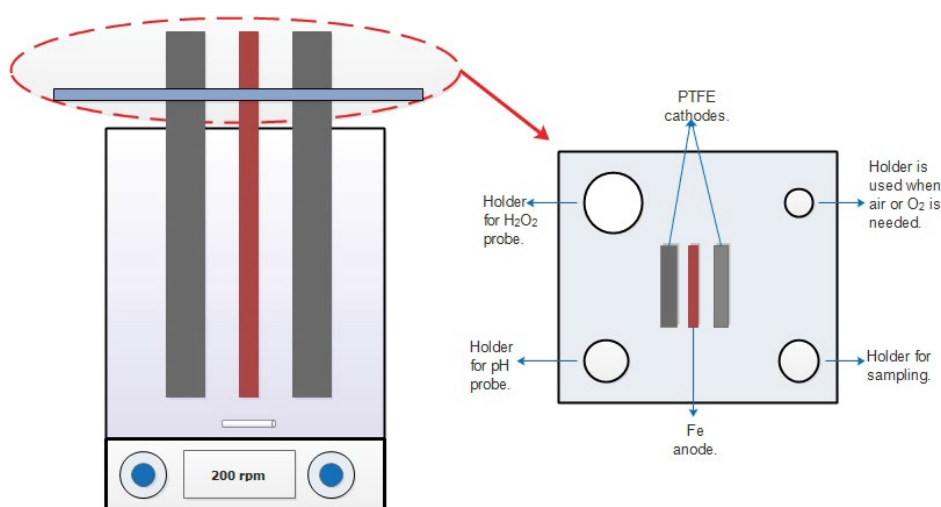


Fig. 1. Designed electrode holder for experimental set-up.

Table 3  
Experiment design and experimental responses of peroxi-coagulation process

Run	A: current density mA/cm <sup>2</sup>	B: initial pH	C: temperature °C	TP (C/C <sub>0</sub> )	MBAS (C/C <sub>0</sub> )	COD (C/C <sub>0</sub> )	TFe mg/L
1	30	7	35	0.10	0.10	0.27	5.80
2	30	7	35	0.08	0.15	0.26	0.90
3	30	3	45	0.04	0.09	0.22	18.20
4	30	7	35	0.13	0.18	0.25	3.70
5	30	11	45	0.61	0.73	0.68	55.40
6	45	3	35	0.05	0.17	0.23	26.40
7	45	7	25	0.07	0.33	0.25	0.90
8	15	7	45	0.20	0.20	0.31	4.70
9	15	7	25	0.10	0.23	0.27	2.20
10	15	11	35	0.72	1.00	0.71	28.80
11	30	11	25	0.64	0.67	0.69	35.10
12	30	3	25	0.02	0.08	0.25	24.80
13	15	3	35	0.03	0.12	0.24	18.80
14	45	11	35	0.51	0.88	0.59	72.20
15	45	7	45	0.06	0.34	0.22	2.90

Table 4  
ANOVA results of fitted quadratic model for TP, MBAS, COD and TFe

Source	Sum of squares	Degrees of freedom	Mean square	F-value	p-value	R <sup>2</sup>	Adj. R <sup>2</sup>
Total phosphorus (TP)							
Model	0.9159	9	0.1018	148.96	<0.0001		
Residual	0.0034	5	0.0007			0.9963	0.9896
Lack of fit	0.0016	3	0.0005	0.6161	0.6671		
Pure error	0.0018	2	0.0009				
Total iron (TFe)							
Model	5,995.25	9	666.14	8.39	0.0153		
Residual	397.13	5	79.43			0.9379	0.8260
Lack of fit	385.04	3	128.35	21.24	0.0453		
Pure error	12.09	2	6.04				
Methylene blue active substances (MBAS)							
Model	1.37	9	0.1521	17.87	0.0027		
Residual	0.0425	5	0.0085			0.9699	0.9156
Lack of fit	0.0391	3	0.0130	7.58	0.1188		
Pure error	0.0034	2	0.0017				
Chemical oxygen demand (COD)							
Model	0.5209	9	0.0579	227.33	<0.0001		
Residual	0.0013	5	0.0003			0.9976	0.9932
Lack of fit	0.0012	3	0.0004	6.69	0.1328		
Pure error	0.0001	2	0.0001				

response. *p*-value of each model (<0.0001, 0.0153, 0.0027, <0.0001 for TP, TFe, MBAS and COD, respectively) were smaller than 0.05 so the models are significant at %95 confidence level. The actual and the predicted values for TP, TFe, MBAS and COD parameters are shown in Fig. 2. It was seen

that there was no significant difference between the measured and predicted values. The correlation coefficients were used to check the goodness of fit of the model. The high values of coefficients for TP ( $R^2 = 0.996$ ), TFe ( $R^2 = 0.937$ ), MBAS ( $R^2 = 0.969$ ) and COD ( $R^2 = 0.997$ ) indicated that responses

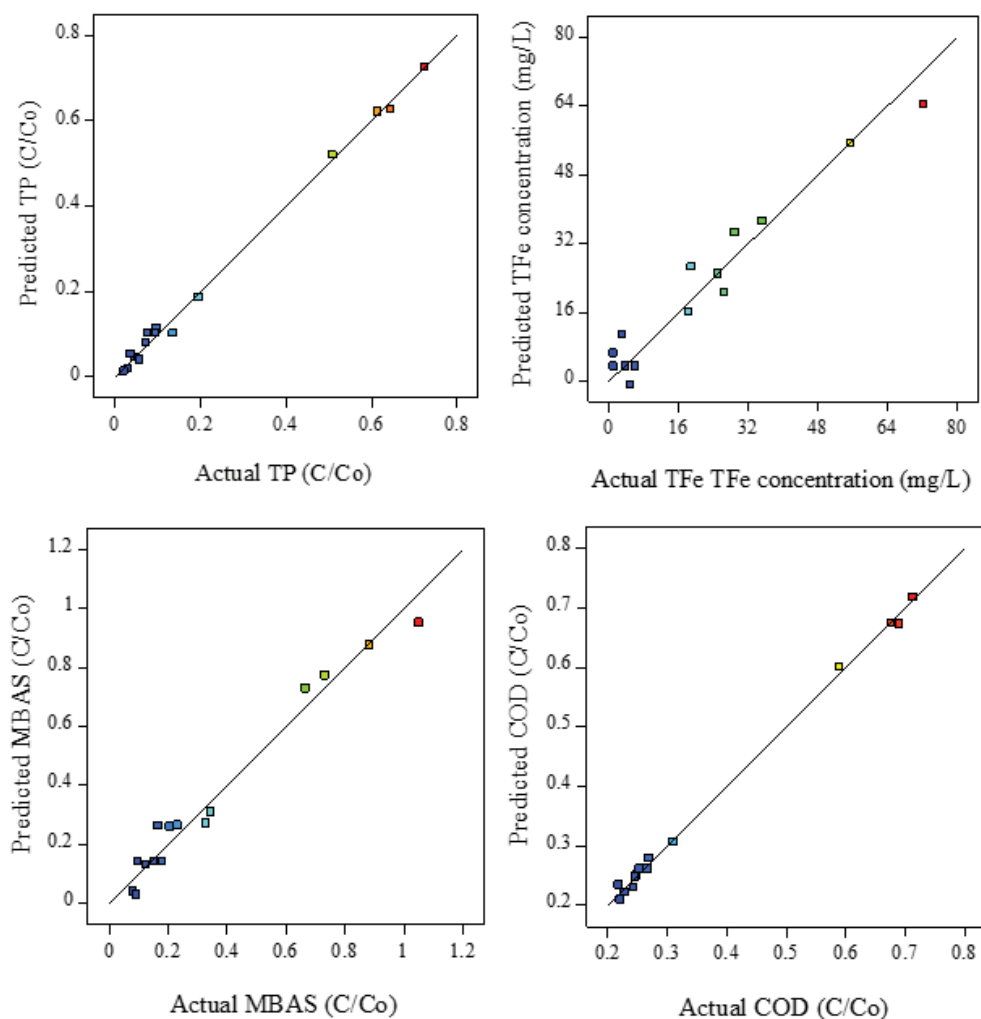


Fig. 2. Predicted vs. actual plots of each response with the application of 30 mA/cm<sup>2</sup>, at pH 7 and 25°C.

could be explained by the models. The values of adjusted  $R^2$  ( $R_a^2$ ) were also high as 0.989, 0.826, 0.915, and 0.993 for TP, TFe, MBAS and COD, respectively. A high  $R_a^2$  value is evidence of high correlation between actual and predicted values of the responses [32].

Individual effects of factors on variables are shown in the perturbation plots (Fig. 3). It is obvious that for all responses, the initial pH ( $B$ ) was the most effective parameter while temperature ( $C$ ) was less effective one. The increase in initial pH showed negative effect on COD, MBAS and TP removal as seen in Figs. 3a–c. As seen from Figs. 3a–c, pH is one of the important parameters affecting the performance of PC process. The optimum pH value was found around 3 in electro-Fenton oxidation processes [24]. Acidic conditions are suitable for the degradation of organic pollutants by the generated reagents that are formed by the conversion of hydrogen ions to hydrogen peroxide with the consumption of dissolved oxygen (Eq. (4)) at pH 3 [33–36]. Also, lower-acidic pH conditions are necessary to avoid Fe precipitation and maintain the kinetics of Fe<sup>2+</sup> conversion to Fe<sup>3+</sup> in the solution [16]. This situation is supported by the TFe concentration shown in Fig. 3d. As seen from the figure, TFe concentration

at pH 3 is higher than at pH 7. This can be due to the Fe<sup>3+</sup> ions forming Fe(OH)<sub>3</sub> flocs which can precipitate and remove the pollutants from wastewater at alkaline pH conditions [24]. In addition, H<sub>2</sub>O<sub>2</sub> decomposes to oxygen and H<sub>2</sub>O that the oxidation potential of <sup>•</sup>OH reduces at neutral pH values. So, at neutral and higher pH values the removal efficiencies of COD, MBAS and TP decreased. The applied current density is an important parameter in EC process. As seen from Fig. 3, the increase in applied current density increased COD and TP removal. This can be due to the high current density delivering more aqueous <sup>•</sup>OH radicals in the bulk solution and also oxidizing ferrous iron to ferric iron [37]. Furthermore, the dissolution of Fe anode increases with the increasing current density and dissolved Fe forms destabilize and aggregate the contaminants present in the effluent [38]. But the increase in current density from 30 to 45 mA/cm<sup>2</sup> negatively affected the MBAS removal. This can be due to more generation of H<sub>2</sub>O<sub>2</sub> that is a scavenger of <sup>•</sup>OH when the applied current density increased beyond a critical value. And also at high current densities hydrogen gas formation on the cathode surface increases. This increment causes the formation of hydrogen bubbles covering electrode surface

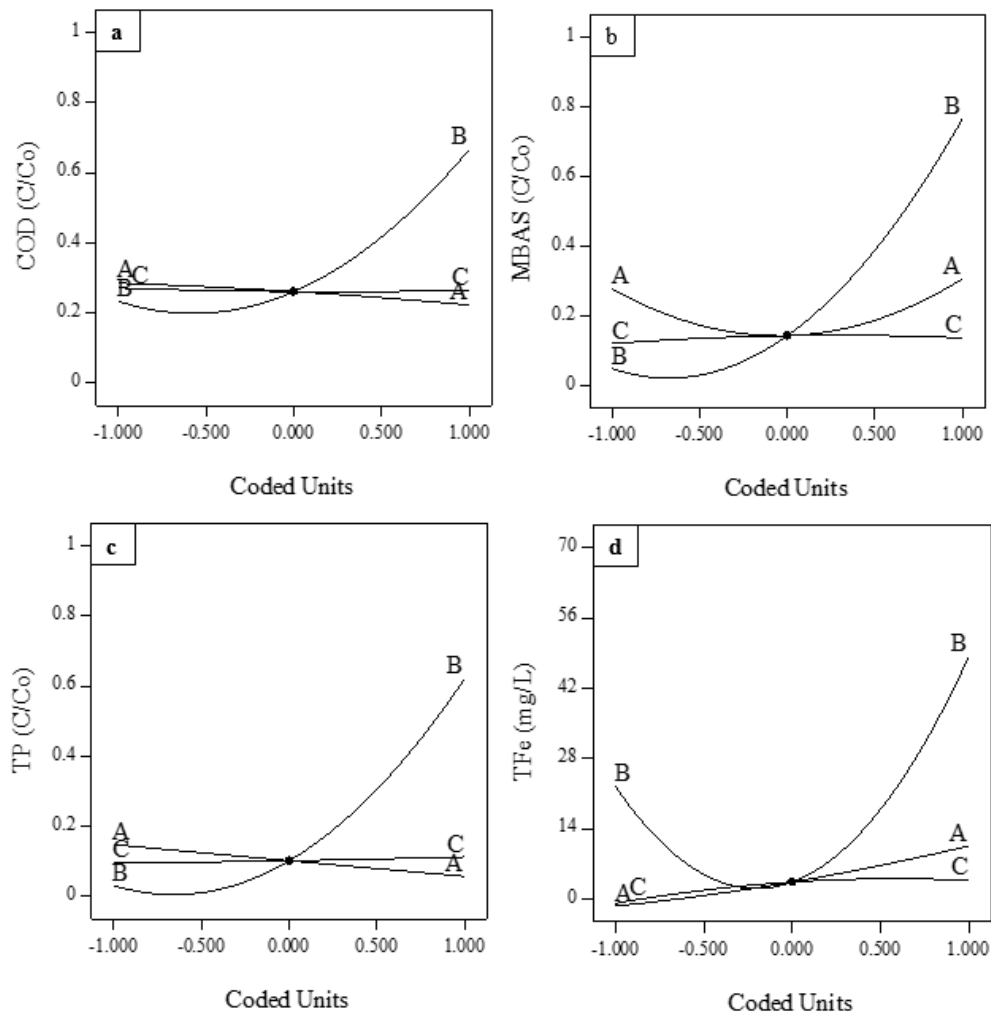


Fig. 3. Perturbation plots for (a) COD, (b) MBAS, (c) TP, and (d) TFe.

and can lower the  $\text{H}_2\text{O}_2$  and  $\cdot\text{OH}$  production [39–41]. The decrease in the rate of oxidation of MBAS can also be due to the hydroperoxyl radicals ( $\text{HO}_2^{\cdot}$ ), produced by the excess ferric ions reacting with  $\text{H}_2\text{O}_2$ , which have much weaker oxidizing power than hydroxyl radicals [17].

TFe concentration (Fig. 3d) was most affected response from the change of initial pH. Since, insoluble iron species  $\text{Fe}(\text{OH})_3$  and  $\text{Fe}(\text{OH})_2$  undergo precipitation between pH 5 and 7, TFe concentration in the bulk solution decreased. However,  $\text{Fe}(\text{OH})^+$ ,  $\text{Fe}(\text{OH})_2$  and  $\text{Fe}(\text{OH})_3^-$  monomeric species are formed at higher pH values and insoluble forms dissolve at those conditions [42,43]. Therefore, in our case, TFe concentration increased as pH value increased after pH 7, which was signified as 0.000-coded unit in Fig. 3d. Moreover, TFe concentration was affected with current density because of the increasing dissolution of the anode at higher current densities.

### 3.2. Effect of controlling factors on responses

A response surface plot, which shows the interaction effects on responses are given in Fig. 4. For each response,

two interactions (*AB* and *BC*) plots were presented since current density-temperature interactions (*AC*) were insignificant statistically and showed a layer shape on the plots.

Normalized value of COD, MBAS and TP responses were given to indicate removal efficiencies during LWWT treatment; however, TFe formation was given in the concentration unit since it was produced during the PC process. The COD removal ratio changed 0.71 to 0.22 as seen from Table 3 and Fig. 4a indicating that this alteration was affected by the interaction of pH-current density and pH-temperature. Low initial pH and high current density provided high COD removal, while temperature had no significant effect on the COD removal. Similarly, MBAS removal was affected mostly from pH changes as seen from Fig. 4b. When pH decreased, MBAS ( $C/C_0$ ) also decreased dramatically at all current density and/or temperature values. MBAS removal ( $C/C_0$ ) reached 0.08 stating 92% MBAS removal efficiency (Table 3) with the application of  $30 \text{ mA/cm}^2$  current density at pH 3 and  $25^\circ\text{C}$ .

It is seen from Fig. 4c, there was no significant change in TP removal ( $C/C_0$ ) arising from the change of the current density and/or temperature at the same pH value.

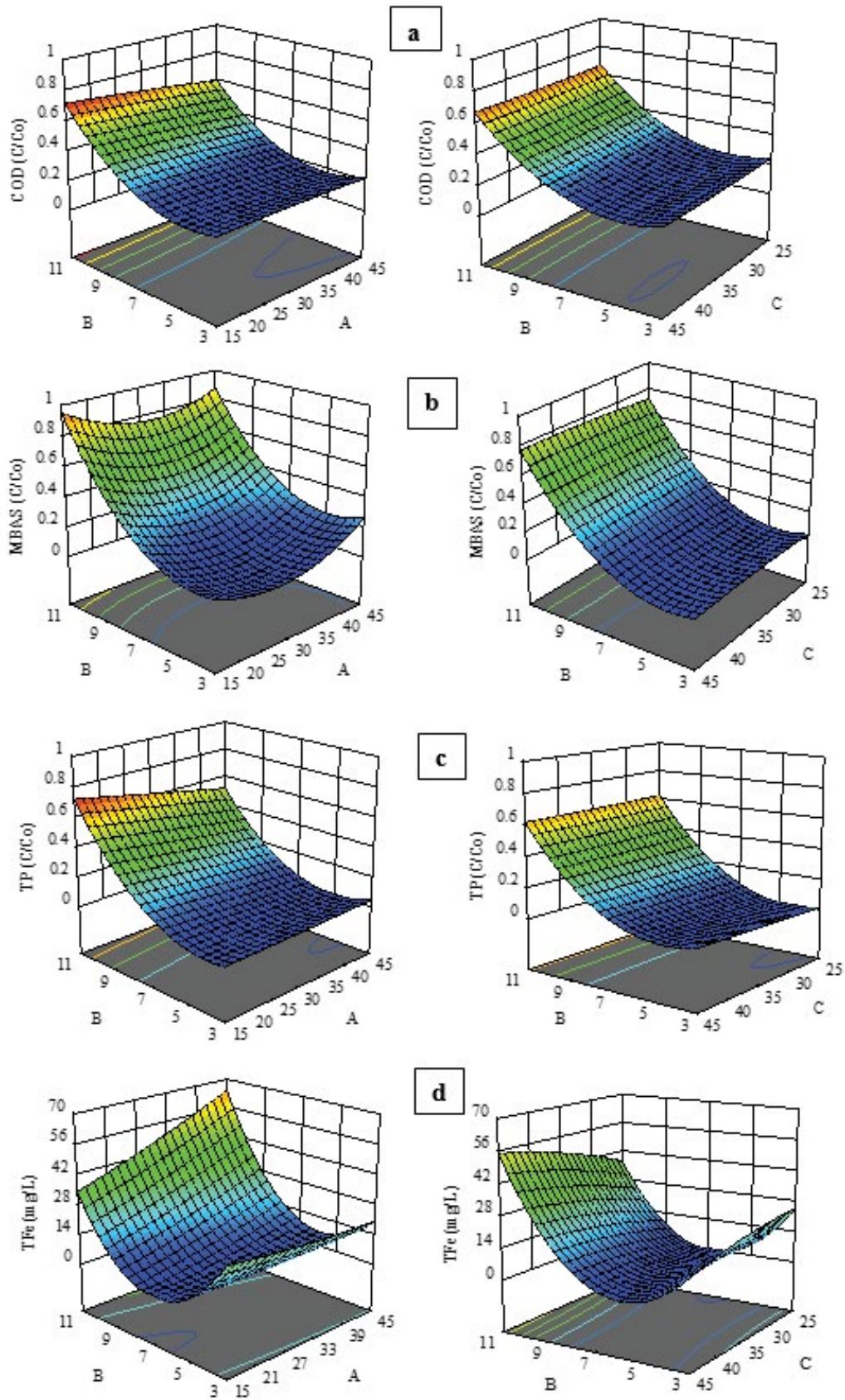


Fig. 4. Response surface plots (a) COD, (b) MBAS, (c) TP, and (d) TFe.

The minimum TP ( $C/C_0$ ) value (0.02) was obtained at pH 3, 30 mA/cm<sup>2</sup> current density and 25°C temperature conditions while the highest TP ( $C/C_0$ ) conditions were obtained at the original pH 11 of LWW as 0.72 (i.e. Run 10 in Table 3).

As another response in the model, TFe also showed a strong relationship with the pH (Fig. 4d). This effect is known to be related to the precipitation behavior of iron depending on pH. Insoluble iron species (such as Fe(OH)<sub>2</sub> and Fe(OH)<sub>3</sub>) occur between pH 6 and 10; outside this pH range, iron species that are dissolved in the bulk solution cause increment in the iron concentration in the effluent.

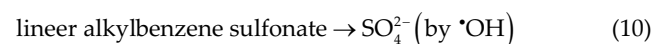
The quadratic model equation for each model was obtained according to design matrix and the responses in Table 3 and the equations were given in coded form (Table 5). As an overall assessment, the interaction of current density/pH (AB) and pH/temperature (BC) were slightly effective for all responses; however, pH change dominated the PC reaction. As described before, pH affects the formation of reagents for the degradation of organic pollutions, maintains the kinetics of Fe<sup>2+</sup> conversion to Fe<sup>3+</sup> ions forming Fe(OH)<sub>3</sub> flocs which can precipitate and remove the pollutants from wastewater.

The aim was to obtain optimal operating conditions for maximum COD, MBAS and TP removal with the established RSM model. On the other hand, dissolved iron in the LWW is not desired due to the formation yellowish tint on the clothes when the LWW is reused. In this context, Run 7 with the application of 45 mA/cm<sup>2</sup> at pH 7 and 25°C resulted in 75%, 67%, and 93% COD, MBAS, and TP removal efficiencies, respectively. In that case, almost no (i.e. 0.90 mg/L) total dissolved iron remained in the bulk solution. This can be due to the H<sub>2</sub>O<sub>2</sub> stability at neutral pH values that avoids the efficient generation of •OH radicals [44]. And also at high pH values dissolved Fe<sup>3+</sup> concentration decrease and inhibits Fe<sup>2+</sup> generation that describes why Fe concentration in the solution is minimum in that process conditions [45].

### 3.3. Effect of oxidants on COD and MBAS treatment

To understand the mechanism of the PC system, formation of H<sub>2</sub>O<sub>2</sub> and S<sub>2</sub>O<sub>8</sub><sup>2-</sup> in the bulk solution during the reaction were followed under best operation conditions (i.e. Run 7). Fig. 5 shows that MBAS and COD removal simultaneously with S<sub>2</sub>O<sub>8</sub><sup>2-</sup> and H<sub>2</sub>O<sub>2</sub> production. As seen from the figure, S<sub>2</sub>O<sub>8</sub><sup>2-</sup> concentration increased with decreasing surfactant concentration and it reached to the maximum value at 20 min of the reaction while MBAS removal was at minimum level. Sulfate concentration arising from linear alkylbenzene sulfonate degradation in reaction (10) [46]

seems to be responsible for the S<sub>2</sub>O<sub>8</sub><sup>2-</sup> increment according to reaction (11) [26].



While S<sub>2</sub>O<sub>8</sub><sup>2-</sup> concentration was increasing between 7–20 min of the reaction, concentration of H<sub>2</sub>O<sub>2</sub> gave a plateau. So that, the decreasing trend in the MBAS and COD treatment indicated that S<sub>2</sub>O<sub>8</sub><sup>2-</sup> formed electrochemically dominate the oxidation of organics during LWW treatment. Barrera-Díaz et al. [47] demonstrated that •OH radicals interact with SO<sub>4</sub><sup>2-</sup> generating the sulfate radical and also the persulfate oxidant. So the presence of SO<sub>4</sub><sup>2-</sup> ions in wastewaters helps the formation of both oxidants for the removal of contaminants [48]. Moreover, it can be said that the decrease in S<sub>2</sub>O<sub>8</sub><sup>2-</sup> concentration after 20 min of the PC reaction depended on the scavenging effect of excess iron according to reaction (8). This can be reason of minor changes in COD and MBAS removal after 20 min of the reaction.

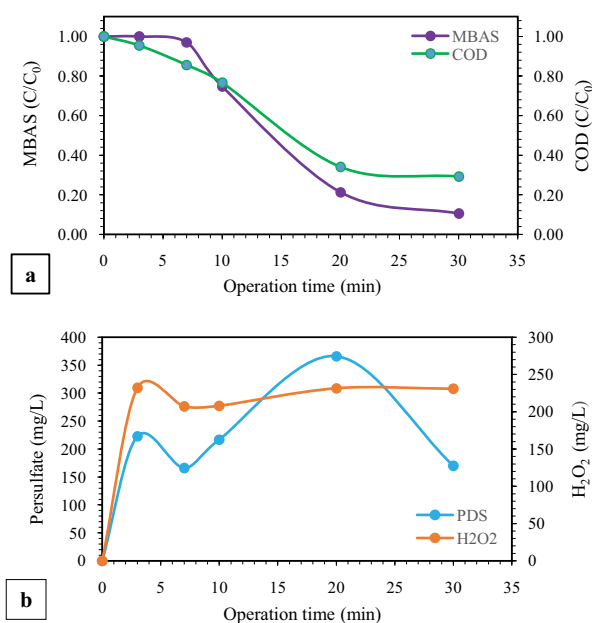


Fig. 5. (a) COD and MBAS removal corresponding with the (b) H<sub>2</sub>O<sub>2</sub> and S<sub>2</sub>O<sub>8</sub><sup>2-</sup> formation during the PC process (current density: 45 mA/cm<sup>2</sup>, pH 7 and 25°C).

Table 5  
Model equations for the removal of MBAS, COD, TP and TFe concentration

	Equations
MBAS ( $C/C_0$ )	$0.1429 + 0.0142 A + 0.3586 B + 0.0081 C - 0.052 AB + 0.0106 AC + 0.0138 BC + 0.1486 A^2 + 0.264 B^2 - 0.0146 C^2$
COD ( $C/C_0$ )	$0.2613 - 0.313 A + 0.2166 B - 0.0033 C - 0.272 AB - 0.017 AC + 0.0035 BC - 0.0071 A^2 + 0.1889 B^2 + 0.0071 C^2$
TP ( $C/C_0$ )	$0.1022 - 0.0452 A + 0.2947 B + 0.0086 C - 0.0576 AB - 0.0281 AC - 0.0116 BC + 0.0009 A^2 + 0.2242 B^2 + 0.0022 C^2$
TFe (mg/L)	$3.47 + 5.99 A + 12.91 B + 2.28 C + 8.95 AB - 0.125 AC + 6.72 BC + 1.19 A^2 + 31.89 B^2 - 1.98 C^2$

A: current density, B: initial pH, and C: temperature.

Table 6  
Treatment of laundry wastewater by the different electrochemical processes

Process	Anode / cathode	pH	Current density	Time (min)	COD removal (%)	Surfactant removal (%)	TP removal (%)	Ref.
EC <sup>a</sup>	Cu/Cu	8.3	26.8 mA/cm <sup>2</sup>	6	72.7	–	–	[2]
EP <sup>b</sup>	C-PTFE	6.3	13.3 mA/cm <sup>2</sup>	120	55	77	–	[3]
EC <sup>c</sup>	Al/Al	6–8	8.8 mA/cm <sup>2</sup>	90	93.2	93.5	96.7	[4]
EC/EF	Al/Ti	6	24.0 mA/cm <sup>2</sup>	10	>80	>95	>95	[49]
EC/EF	Al/Al	5.1	5.0 V	40	62	–	–	[9]
PEC <sup>d</sup>	Fe/Fe	5	0.50 mA/cm <sup>2</sup>	10	–	81.6	–	[24]
PO <sup>e</sup>	–	3–3.5	–	180	59.1	>95.5	74.7	[5]
AOP <sup>f</sup>	–	7	–	55	–	96	–	[50]
PC <sup>g</sup>	Fe/C-PTFE	7	45.0 mA/cm <sup>2</sup>	30	75	67	100	This study

<sup>a</sup>Electrocoagulation, <sup>b</sup>Electroperoxone, <sup>c</sup>Electrocoagulation/Electroflotation, <sup>d</sup>Peroxi-electrocoagulation, <sup>e</sup>Photocatalytic ozonation, <sup>f</sup>Advanced oxidation process, <sup>g</sup>Peroxi-coagulation

### 3.4. Energy and electrode consumptions

Energy and electrode consumptions are the main operating costs of PC. Therefore, cost of PC process was calculated with the following equations:

$$C_{\text{energy}} \left( \text{kWh} / \text{m}^3 \right) = \frac{U i t}{V} \quad (12)$$

Energy consumption was calculated with Eq. (12) where  $U$  is an average cell voltage (V),  $i$  is a current (A),  $t$  is operating time (h) and  $V$  is volume of PC reactor (m<sup>3</sup>).

$$C_{\text{electrode}} \left( \text{kg} / \text{m}^3 \right) = \frac{i t M_w}{z F V} \quad (13)$$

Electrode consumption was calculated with Eq. (13), where  $M_w$  is molecular weight of iron (g/mol),  $z$  is a number of electrons involved in the process (2 for Fe), and  $F$  is Faraday constant (96,485 C/mol).

Unit electrical price was taken as 0.085 €/kWh for the Turkish Market, September 2019. The iron electrode material price was 0.48 €/kg. As a result, the overall operating cost was found to be 2,49 Euro/m<sup>3</sup> for the optimum conditions.

## 4. Conclusion

PC process was developed with carbon-PTFE and iron electrodes to determine the optimal treatment conditions for LWW by using response surface methodology. Treatment process with PC depends on the in-situ H<sub>2</sub>O<sub>2</sub> production by carbon-PTFE cathodes and ferrous iron generation by iron sheet anode. Under optimal conditions which means maximum treatment efficiency with minimum residual TFe concentration: pH was 7, the applied current density was 45 mA/cm<sup>2</sup> and temperature was 25°C, 75% of COD, 67% of MBAS and nearly 100% TP removal were achieved. Whereas the change of temperature was insignificant, pH change dominated the course of the reaction. To evaluate the process mechanism, S<sub>2</sub>O<sub>8</sub><sup>2-</sup> and H<sub>2</sub>O<sub>2</sub> were followed under optimal conditions. H<sub>2</sub>O<sub>2</sub> produced by oxygen reduction at

the cathode surface due to carbon-PTFE. Furthermore, S<sub>2</sub>O<sub>8</sub><sup>2-</sup> concentration was also noteworthy which is produced with degradation of linear alkyl benzene sulfonate in the LWW.

When the removal efficiencies in other chemical processes are compared in Table 6, it is seen that EC process is the most effective for LWW. COD and TP removal efficiencies in this study (PC) are as well as EC process but surfactant removal efficiencies are not as good as EC process. But, in-situ oxidant production in the PC process is the main advantage when compared with the EC process. So, it can be said that PC process can be used for the treatment of LWW as an alternative treatment method.

## Acknowledgment

This research is supported by the Scientific and Technological Research Council of Turkey (TUBITAK) [grant number: 115Y797].

## References

- [1] K. Sheth, M.D. Desai, M. Patel, K. Sheth, M.D. Desai, M. Patel, A study on characterization and treatment of laundry effluent, *Int. J. Innovative Res. Sci. Technol.*, 4 (2017) 50–55.
- [2] C. Yun, D. Kim, W. Kim, D. Son, D. Chang, J. Kim, Y. Bae, H. Bae, Y. Sunwoo, M. Kwak, Application and assessment of enhanced electrolytic process for laundry wastewater treatment, *Int. J. Electrochem. Sci.*, 9 (2014) 1522–1536.
- [3] O. Turkey, S. Barişçi, M. Sillanpää, E-peroxone process for the treatment of laundry wastewater: a case study, *J. Environ. Chem. Eng.*, 5 (2017) 4282–4290.
- [4] F. Janpoor, A. Torabian, V. Khatibikamal, Treatment of laundry waste-water by electrocoagulation, *J. Chem. Technol. Biotechnol.*, 86 (2011) 1113–1120.
- [5] D.I. Kern, R.d.O. Schwaickhardt, G. Mohr, E.A. Lobo, L.T. Kist, Ê.L. Machado, Toxicity and genotoxicity of hospital laundry wastewaters treated with photocatalytic ozonation, *Sci. Total Environ.*, 443 (2013) 566–572.
- [6] J.K. Braga, M.B.A. Varesche, Commercial laundry water characterisation, *Am. J. Anal. Chem.*, 5 (2014) 8.
- [7] F.-J. Zhu, W.-L. Ma, T.-F. Xu, Y. Ding, X. Zhao, W.-L. Li, L.-Y. Liu, W.-W. Song, Y.-F. Li, Z.-F. Zhang, Removal characteristic of surfactants in typical industrial and domestic wastewater treatment plants in Northeast China, *Ecotoxicol. Environ. Saf.*, 153 (2018) 84–90.

- [8] S. Bering, J. Mazur, K. Tarnowski, M. Janus, S. Mozia, A.W. Morawski, The application of moving bed bio-reactor (MBBR) in commercial laundry wastewater treatment, *Sci. Total Environ.*, 627 (2018) 1638–1643.
- [9] C.-T. Wang, W.-L. Chou, Y.-M. Kuo, Removal of COD from laundry wastewater by electrocoagulation/electroflotation, *J. Hazard. Mater.*, 164 (2009) 81–86.
- [10] F.J. Beltran, J.F. Garcia-Araya, P.M. Alvarez, Sodium dodecylbenzenesulfonate removal from water and wastewater. 1. Kinetics of decomposition by ozonation, *Ind. Eng. Chem. Res.*, 39 (2000) 2214–2220.
- [11] S. Šostar-Turk, I. Petrinčić, M. Simonič, Laundry wastewater treatment using coagulation and membrane filtration, *Resour. Conserv. Recycl.*, 44 (2005) 185–196.
- [12] X. Shang, H.-C. Kim, J.-H. Huang, B.A. Dempsey, Coagulation strategies to decrease fouling and increase critical flux and contaminant removal in microfiltration of laundry wastewater, *Sep. Purif. Technol.*, 147 (2015) 44–50.
- [13] E. Brillas, R. Sauleda, J. Casado, Peroxi-coagulation of aniline in acidic medium using an oxygen diffusion cathode, *J. Electrochem. Soc.*, 144 (1997) 2374–2379.
- [14] E. Brillas, R. Sauleda, J. Casado, Degradation of 4-chlorophenol by anodic oxidation, electro-Fenton, photoelectro-Fenton, and peroxi-coagulation processes, *J. Electrochem. Soc.*, 145 (1998) 759–765.
- [15] A. Kumar, P. Nidheesh, M.S. Kumar, Composite wastewater treatment by aerated electrocoagulation and modified peroxi-coagulation processes, *Chemosphere*, 205 (2018) 587–593.
- [16] S. Vasudevan, An efficient removal of phenol from water by peroxi-electrocoagulation processes, *J. Water Process Eng.*, 2 (2014) 53–57.
- [17] E. Brillas, B. Boye, M.A. Banos, J.C. Calpe, J.A. Garrido, Electrochemical degradation of chlorophenoxy and chlorobenzoic herbicides in acidic aqueous medium by the peroxi-coagulation method, *Chemosphere*, 51 (2003) 227–235.
- [18] B. Boye, E. Brillas, M.M. Dieng, Electrochemical degradation of the herbicide 4-chloro-2-methylphenoxyacetic acid in aqueous medium by peroxi-coagulation and photoperoxi-coagulation, *J. Water Process Eng.*, 540 (2003) 25–34.
- [19] G. Ren, M. Zhou, P. Su, L. Liang, W. Yang, E. Mousset, Highly energy-efficient removal of acrylonitrile by peroxi-coagulation with modified graphite felt cathode: Influence factors, possible mechanism, *J. Water Process. Eng.*, 343 (2018) 467–476.
- [20] D. Salari, A. Niaei, A. Khataee, M. Zarei, Electrochemical treatment of dye solution containing CI Basic Yellow 2 by the peroxi-coagulation method and modeling of experimental results by artificial neural networks, *J. Electroanal. Chem.*, 629 (2009) 117–125.
- [21] M. Zarei, A. Niaei, D. Salari, A. Khataee, Application of response surface methodology for optimization of peroxi-coagulation of textile dye solution using carbon nanotube-PTFE cathode, *J. Hazard. Mater.*, 173 (2010) 544–551.
- [22] M. Zarei, A. Niaei, D. Salari, A.R. Khataee, Removal of four dyes from aqueous medium by the peroxi-coagulation method using carbon nanotube-PTFE cathode and neural network modeling, *J. Electroanal. Chem.*, 639 (2010) 167–174.
- [23] M. Zarei, D. Salari, A. Niaei, A. Khataee, Peroxi-coagulation degradation of CI Basic Yellow 2 based on carbon-PTFE and carbon nanotube-PTFE electrodes as cathode, *Electrochim. Acta*, 54 (2009) 6651–6660.
- [24] E. Yüksel, İ.A. Şengil, M. Özacar, The removal of sodium dodecyl sulfate in synthetic wastewater by peroxi-electrocoagulation method, *Chem. Eng. J.*, 152 (2009) 347–353.
- [25] E. Brillas, J. Casado, Aniline degradation by electro-Fenton® and peroxi-coagulation processes using a flow reactor for wastewater treatment, *Chemosphere*, 47 (2002) 241–248.
- [26] K.C.d.F. Araújo, J.P.d.P. Barreto, J.C. Cardozo, E.V. dos Santos, D.M. de Araújo, C.A. Martínez-Huitle, Sulfate pollution: evidence for electrochemical production of persulfate by oxidizing sulfate released by the surfactant sodium dodecyl sulfate, *Environ. Chem. Lett.*, 16 (2018) 647–652.
- [27] H. Chen, Z. Zhang, M. Feng, W. Liu, W. Wang, Q. Yang, Y. Hu, Degradation of 2, 4-dichlorophenoxyacetic acid in water by persulfate activated with FeS (mackinawite), *Chem. Eng. J.*, 313 (2017) 498–507.
- [28] S. Waclawek, H.V. Lutze, K. Grübel, V.V. Padil, M. Černík, D.D. Dionysiou, Chemistry of persulfates in water and wastewater treatment: a review, *Chem. Eng. J.*, 330 (2017) 44–62.
- [29] L.W. Matzek, K.E. Carter, Activated persulfate for organic chemical degradation: a review, *Chemosphere*, 151 (2016) 178–188.
- [30] APHA, WPCF, Standard Methods for the Examination of Water and Wastewater, 20, 1998.
- [31] K.-C. Huang, R.A. Couttenye, G.E. Hoag, Kinetics of heat-assisted persulfate oxidation of methyl tert-butyl ether (MTBE), *Chemosphere*, 49 (2002) 413–420.
- [32] O. Turkey, S. Barisci, A. Dimoglo, Assessment of parameters influencing the electro activated water character and explanation of process mechanism, *Process Saf. Environ.*, 99 (2016) 129–136.
- [33] F. Ghanbari, M. Moradi, A comparative study of electrocoagulation, electrochemical Fenton, electro-Fenton, and peroxi-coagulation for decolorization of real textile wastewater: electrical energy consumption and biodegradability improvement, *J. Environ. Chem. Eng.*, 3 (2015) 499–506.
- [34] A.A. Burbano, D.D. Dionysiou, M.T. Suidan, T.L. Richardson, Oxidation kinetics and effect of pH on the degradation of MTBE with Fenton reagent, *Water Res.*, 39 (2005) 107–118.
- [35] J. Li, Z. Luan, L. Yu, Z. Ji, Pretreatment of acrylic fiber manufacturing wastewater by the Fenton process, *Desalination*, 284 (2012) 62–65.
- [36] P.V. Nidheesh, R. Gandhimathi, Trends in electro-Fenton process for water and wastewater treatment: an overview, *Desalination*, 299 (2012) 1–15.
- [37] O. Turkey, Z.G. Ersoy, S. Barışçı, The application of an electroperoxone process in water and wastewater treatment, *J. Electrochem. Soc.*, 164 (2017) E94–E102.
- [38] A.S. Fajardo, R.F. Rodrigues, R.C. Martins, L.M. Castro, R.M. Quinta-Ferreira, Phenolic wastewaters treatment by electrocoagulation process using Zn anode, *Chem. Eng. J.*, 275 (2015) 331e341.
- [39] X. Li, Y. Wang, J. Zhao, H. Wang, B. Wang, J. Huang, S. Deng, G. Yu, Electro-peroxone treatment of the antidepressant venlafaxine: operational parameters and mechanism, *J. Hazard. Mater.*, 300 (2015) 298–306.
- [40] W. Yao, X. Wang, H. Yang, G. Yu, S. Deng, J. Huang, B. Wang, Y. Wang, Removal of pharmaceuticals from secondary effluents by an electro-peroxone process, *Water Res.*, 88 (2016) 826–835.
- [41] K. Bouzek, I. Roušar, M. Taylor, Influence of anode material on current yield during ferrate (VI) production by anodic iron dissolution Part II: current efficiency during anodic dissolution of white cast iron to ferrate (VI) in concentrated alkali hydroxide solutions, *J. Appl. Electrochem.*, 26 (1996) 925–931.
- [42] C.A. Martínez-Hustle, E. Brillas, Decontamination of wastewaters containing synthetic organic dyes by electrochemical methods: a general review, *Appl. Catal., B*, 87 (2009) 105–145.
- [43] T. Yılmaz Nayır, S. Kara, Container washing wastewater treatment by combined electrocoagulation–electrooxidation, *Sep. Sci. Technol.*, 53 (2018) 1592–1603.
- [44] E.do. Vale-Júnior, D.R. da Silva, A.S. Fajardo, C.A. Martínez-Hustle, Treatment of an azo dye effluent by peroxi-coagulation and its comparison to traditional electrochemical advanced processes, *Chemosphere*, 204 (2018) 548–555.
- [45] A.R. Yazdanbakhsh, M.R. Massoudinegad, S. Elias, A.S. Mohammadi, The influence of operational parameters on reducing of azithromycin COD from wastewater using the peroxi-electrocoagulation process, *J. Water Process Eng.*, 6 (2015) 51–57.
- [46] A. Arslan, E. Topkaya, S. Veli, D. Bingöl, Optimization of ultrasonication process for the degradation of linear alkyl benzene sulfonic acid by response surface methodology, *CLEAN-Soil, Air, Water*, (2018), <https://doi.org/10.1002/clen.201700508>.
- [47] C. Barrera-Díaz, P. Cañizares, F. Fernández, R. Natividad, M. Rodrigo, Electrochemical advanced oxidation processes: an overview of the current applications to actual industrial effluents, *J. Mex. Chem. Soc.*, 58 (2014) 256–275.
- [48] E. Brillas, C.A. Martínez-Hustle, Decontamination of wastewaters containing synthetic organic dyes by electrochemical

- methods. An updated review, *Appl. Catal., B*, 166 (2015) 603–643.
- [49] J. Ge, J. Qu, P. Lei, H. Liu, New bipolar electrocoagulation–electroflotation process for the treatment of laundry wastewater, *Sep. Purif. Technol.*, 36 (2004) 33–39.
- [50] A. Arslan, E. Topkaya, D. Bingöl, S. Veli, Removal of anionic surfactant sodium dodecyl sulfate from aqueous solutions by  $O_3/UV/H_2O_2$  advanced oxidation process: process optimization with response surface methodology approach, *Sustainable Environ. Res.*, 28 (2018) 65–71.